modelling

MDPI

Communication

The Impact of the Polymer Layer Thickness in the Foundation Shim on the Stiffness of the Multi-Bolted Foundation Connection

Rafał Grzejda

Faculty of Mechanical Engineering and Mechatronics, West Pomeranian University of Technology in Szczecin, al. Piastow 19, 70-310 Szczecin, Poland; rafal.grzejda@zut.edu.pl

Abstract: Finite element modelling of multi-bolted foundation connections used for the foundation of heavy machinery or equipment is presented. Connections made using different types of shims, with particular emphasis on polymer–steel shims, are investigated. The stiffness characteristics for the adopted models of multi-bolted foundation connections at the installation stage are described and compared. It is shown that the use of polymer–steel shims can result in a significant improvement in the stiffness of a multi-bolted foundation connection compared to a connection with a polymer shim, and in achieving a multi-bolted foundation connection with a stiffness similar to that of a connection with a steel shim (at a sufficiently low polymer layer thickness).

Keywords: multi-bolted foundation connection; stiffness; foundation cast shim; EPY resin compound; finite element method

Citation: Grzejda, R. The Impact of the Polymer Layer Thickness in the Foundation Shim on the Stiffness of the Multi-Bolted Foundation Connection. *Modelling* **2024**, *5*, 1365–1374. https://doi.org/10.3390/modelling5040070

Academic Editor: Abílio M. P. De Jesus

Received: 30 August 2024
Revised: 11 September 2024
Accepted: 25 September 2024
Published: 26 September 2024

1. Introduction

Multi-bolted connections are used in many industries and in various types of constructions [1–3]. They are most often applied to join machined components, i.e., those with a defined geometric texture on the surfaces to be joined [4,5]. In some cases, such as the seating of heavy machinery and equipment—for example, marine engines [6–8]—this texture, but also the mutual positioning of the surfaces of the components to be joined, is decisive for the correctness of the completed assembly [9–11]. One way of circumventing the difficulties encountered during machine seating is to use special cast shims [12,13]. The idea of cast shims is also applied, for example, to bolted connections used in aerospace structures [14–19] and to prevent geometric imperfections arising during the assembly of classic bolted flange connections [20]. In all of the aforementioned cases, the use of cast shims creates a kind of composite structure combining steel or aluminium components and polymer. Modelling such structures can answer many questions about the influence of the properties of the cast shims on the mechanical characteristics of the multi-bolted connection. It also fits perfectly into the trend of modelling composite structures, which are present in many areas of human activity [21–24].

Traditional shims used in the seating of machinery can be made of steel or cast polymer [25,26]. The use of steel shims is related to the need to ensure that the pressure on all shims is evenly distributed by matching their surfaces with the retaining surfaces of the machine to be installed and the foundation. Such operations are difficult, tedious and labour-intensive. In addition, in this case of seating, the use of the preloading of foundation bolts results in significant contact distortion between the components to be joined [10]. When cast polymer shims are used, the aforementioned difficulties for machine seating do not occur. In this case, precise machining of the surfaces of the components to be joined is not necessary. Furthermore, the direct casting of the shims under the machine base ensures that the joined surfaces of these components fit closely together. Irregularities resulting from the roughness of the surfaces to be joined are filled in with polymer, so that the

pressure distribution on these surfaces is more favourable than in the case of seating using steel shims [27]. In addition, the polymer shims are structural elements that provide good thermal and acoustic insulation for the supported steel or cast iron machine structure [28]. However, a disadvantage of seating with cast polymer shims is that they creep under service conditions, causing preload relaxation in the foundation bolts [9,29].

The existing literature still pays little attention to the study and modelling of bolted foundation connections. Grudziński and Konowalski [30] analysed the flexibility of a steel adjustable foundation shim based on experimental tests on a testing machine. A continuation of these experimental studies is described in papers [10,11] for the case of steel and polymer shims. Yongsheng et al. [31] dealt with contact stiffness calculations of bed–foundation interfaces, taking into account foundation creep for connections containing a shim plate. An analysis of the change from steel to polymer shims for the foundation of marine power plant mechanisms is presented in [27]. The initial research on steel–polymer shims was published by Piaseczny [9,32], who died prematurely. In contrast, the finite element method (FEM) models used are most often concerned with systems in which the object in question is anchored by foundation bolts to the ground without the presence of shims [33–35]. The above conclusions from the literature review mandate the undertaking of FEM analyses of multi-bolted foundation connections. This communication aims to develop an understanding of the impact of the thickness of the polymer layer in the foundation shim on the stiffness of the multi-bolted foundation connection. This issue has not previously been described in the available literature and constitutes the novelty of this communication. The EPY resin compound was used as a polymer material, as this is a material successfully used in the seating of machinery and equipment [12,13].

2. Materials and Methods

2.1. Fundamentals of Analysis

In the modelling of fasteners in bolted connections, simplifications are sought that speed up the calculation process and do not affect the accuracy of the results within the phenomena being analysed. This means that, depending on the modelling objective (i.e., the specified boundary conditions at which the behaviour of the connection is checked), it is possible to use simplified fastener models in the bolted connection model. This approach is particularly valid when the stiffness of the joined components in a multi-bolt connection is being analysed. An overview of simplified methods for modelling fasteners in bolted connections is included, for example, in [36–38]. Simplified modelling uses, among other things, models in the form of composite cylinders of variable diameter replacing the bolt head and its shank and nut [39–41] or only cylinders replacing the bolt head and nut, without including the entire bolt shank [42,43], but also models without overt bolt participation [44]. In this article, the second approach mentioned above was used to model the bolts in a multi-bolted connection.

One of the important issues taken into account in the calculation of multi-bolted foundation connections is the analysis of the stiffness of their components. Treating bolts as linear type elements, their elastic flexibility can be determined using the instructions given in the VDI 2230 standard [45] or by a simplified method [46]. Therefore, the determination of bolt stiffness is not dealt with in this communication. However, there is no equally easy way to determine the elastic flexibility of components joined in multi-bolted foundation connections. Therefore, the finite element method is usually used to determine it precisely.

To analyse the deposition methods mentioned in the introduction, calculations were performed for the following models:

- FEM-S—model with steel shim;
- FEM-P—model with polymer shim;
- FEM-PS*n*—model with polymer–steel shim with polymer layer thickness equal to *n* (for n = 1, 2, 3, 4, 5).

This communication examines the cross-section of a multi-bolted foundation connection with the single-joint geometry, presented in schematic form in Figures 1–3. The

bolted joint was formed of two steel plates, (2) and (4), representing sections of the machine base and the continuous footing. The shims, (3) and (6), corresponding to the seating method used, were placed between the plates. As the purpose of this communication is to analyse the stiffness of the joined components, the full bolt model was not included in the connection. The bolt was represented in this case by stamp (1) and the nut by stamp (5). The diameter of these punches was 46 mm and corresponded to the pressure area of the M30 nut.

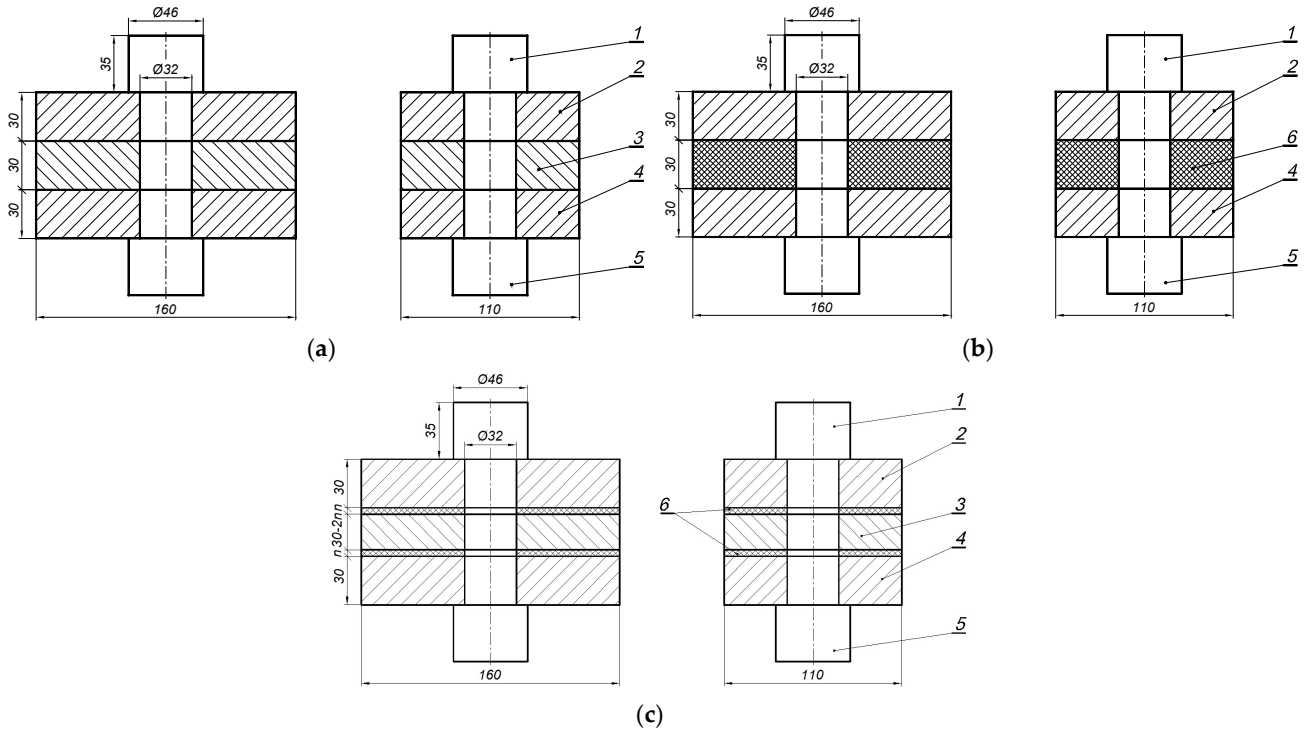

Figure 1. Geometry of bolted foundation joint model with (**a**) steel shim; (**b**) polymer shim; (**c**) and polymer–steel shim (1—bolt head; 2—top plate; 3—steel shim; 4—bottom plate; 5—nut; 6—polymer shim). Dimensions shown on sketches are in mm.

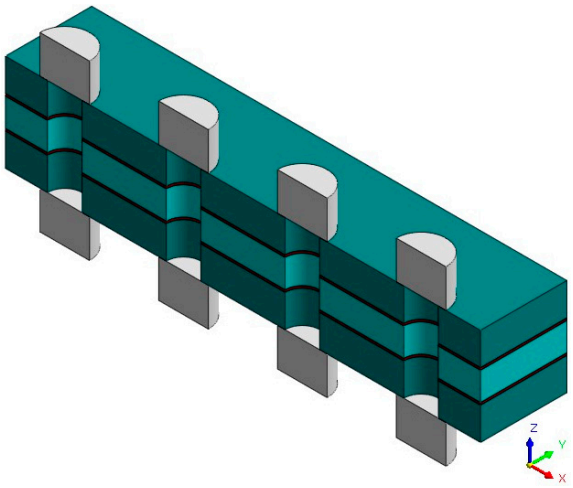

Figure 2. A 3D model of the multi-bolted foundation connection with the polymer–steel shim.

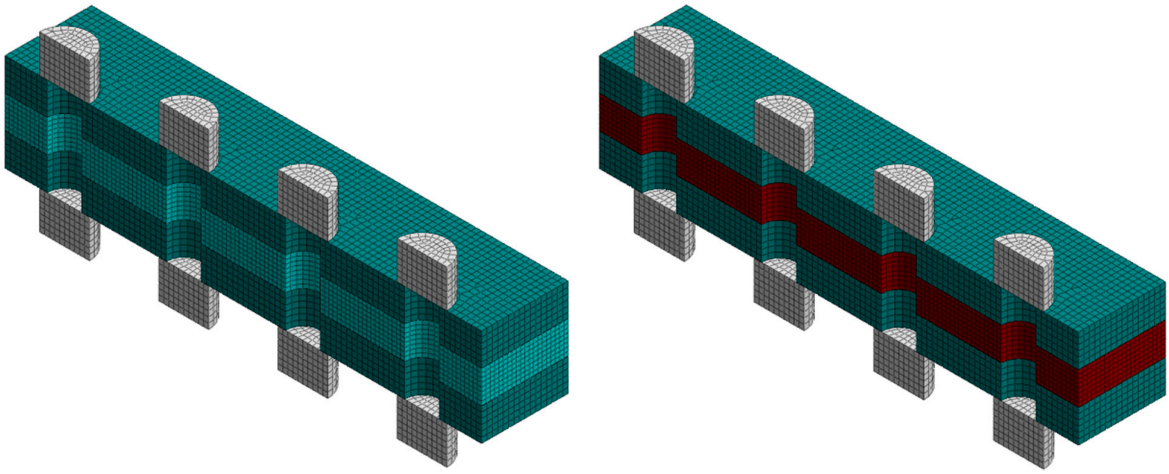

(**a**) (**b**)

Figure 3. Models of multi-bolted foundation connection with (**a**) steel shim and (**b**) polymer shim.

2.2. FEM-Based Models

Calculations were carried out for the dimensions of the components to be joined, as shown in Figure 1. The EPY resin compound was assumed to be a linear material (based on [47,48]). The material constants for the materials used in the models, including the elastic modulus E and Poisson's ratio ν, are listed in Table 1.

Table 1. Characteristics of materials used for foundation shims.

Material	*E*, GPa	ν
Steel	210	0.3
EPY	7.5	0.376

Because of the plane of symmetry occurring in the considered cross-section of the multi-bolted foundation connection, only half of the connection was taken into account in the calculations (see Figure 2).

FEM-based connection models created in Midas NFX 2023 R1 software [49] are shown for all the seating methods adopted in Figures 3 and 4. A 'rough' contact joint model was applied between the steel joined components and the steel shim (for a review, see [50]). Simultaneously, a 'welded' model of the contact joint between the steel joined components and the polymer shim was applied.

The following parameters were adopted for the 'rough' contact joint model:

- Normal stiffness scaling factor—10;
- Tangential stiffness scaling factor—1;
- Coefficient of static friction—0.6.

The 'welded' contact elements applied prevented movement of the components relative to each other in any direction, according to the actual execution of the multi-bolted foundation connection [49].

For all models, a 'hybrid mesher' generator was used to create the finite element mesh. It was assumed that the side length of the finite element for the joined components and the bolt head and nut must be less than 5 mm. Conversely, for the steel shim and polymer shim, it was assumed to be less than 4 mm. The size of the finite elements for the polymer layer in the polymer–steel shim was taken in such a way that there were at least two finite element layers.

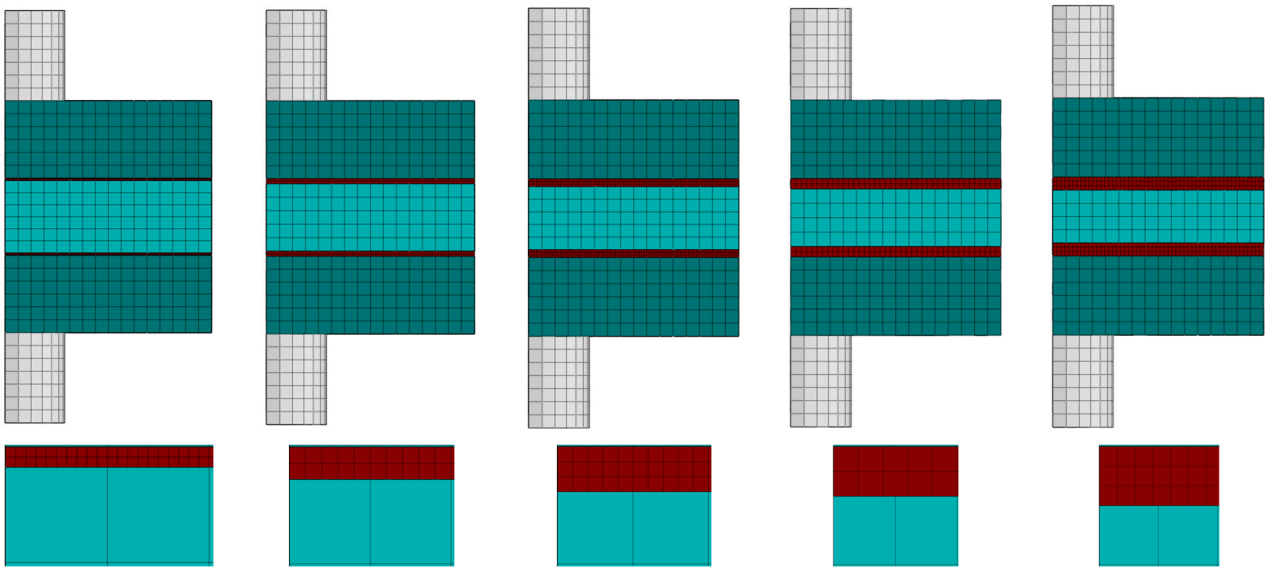

Figure 4. Models of the multi-bolted foundation connection with the polymer–steel shim for (**a**) n = 1; (**b**) n = 2; (**c**) n = 3; (**d**) n = 4; and (**e**) n = 5 (view in the Z0Y plane).

Spatial finite elements were used to build the model meshes. The mesh characteristics of the whole models are summarised in Table 2.

Table 2. Mesh characteristics of multi-bolted foundation connection models.

Model	Number of Finite Elements	Number of Nodes
FEM-S	43,432	44,625
FEM-PS1	580,992	838,248
FEM-PS2	173,296	235,457
FEM-PS3	239,160	301,041
FEM-PS4	66,808	84,701
FEM-PS5	124,120	154,159
FEM-P	43,272	44,539

The individual models were fixed at nodes on the back side of the nut in the direction of the bolt axis and loaded by normal forces at nodes on the top surface of the bolt head. Boundary conditions resulting from the symmetry of the connections were also introduced in the models. With the above boundary and loading conditions, the joined components in the multi-bolted foundation connection models were subjected to compression, which is in line with the actual performance of these connections.

Calculations were conducted with a non-linear solver in ten steps with an incrementally increasing load F from 0 to 200 kN. Non-linear static analyses were performed in all cases.

3. Results and Discussion

Example calculation results for the adopted FEM-based models for displacements in the Z0X plane under a 200 kN load are shown in Figures 5 and 6.

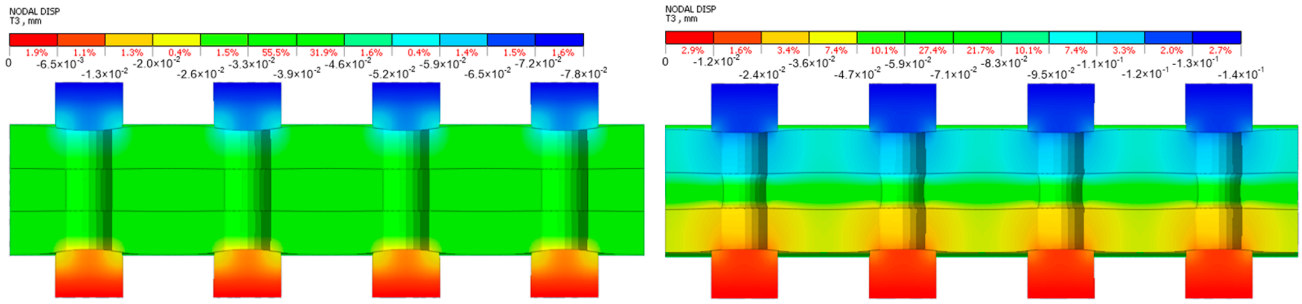

(**a**) (**b**)

Figure 5. Displacements in the Z0X plane of the multi-bolted foundation connection model under the action of a force of 200 kN for (**a**) the FEM-S model and (**b**) the FEM-P model.

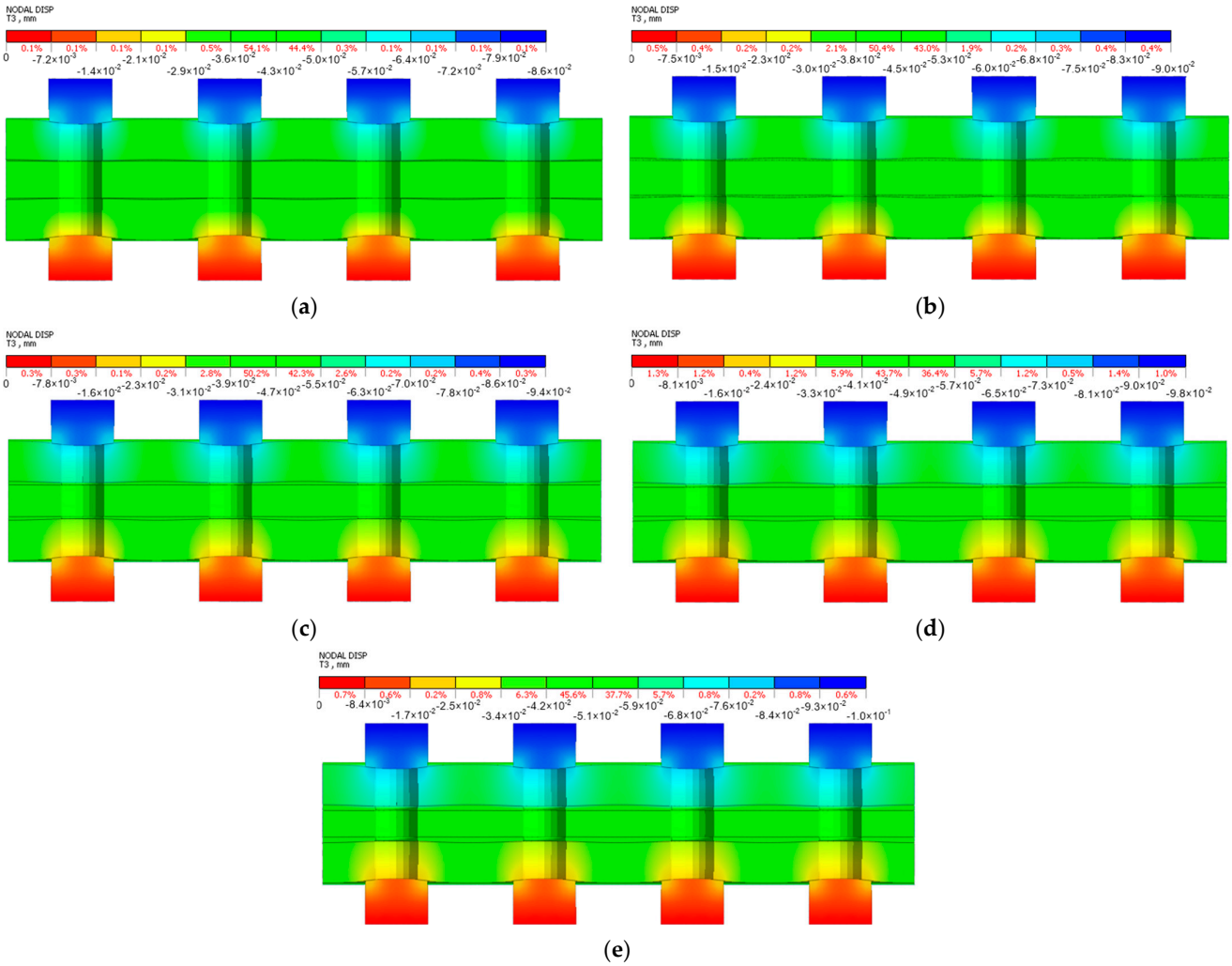

(**a**) (**b**)

(**c**) (**d**)

(**e**)

Figure 6. Displacements in the Z0X plane of the multi-bolted foundation connection model under the action of a force of 200 kN for (**a**) the FEM-PS1 model; (**b**) the FEM-PS2 model; (**c**) the FEM-PS3 model; (**d**) the FEM-PS4 model; and (**e**) the FEM-PS5 model.

For the purpose of the comparative analysis of the computational results, a proper comparison was made between the results obtained for all FEM-based models of the connection under study (Figure 7).

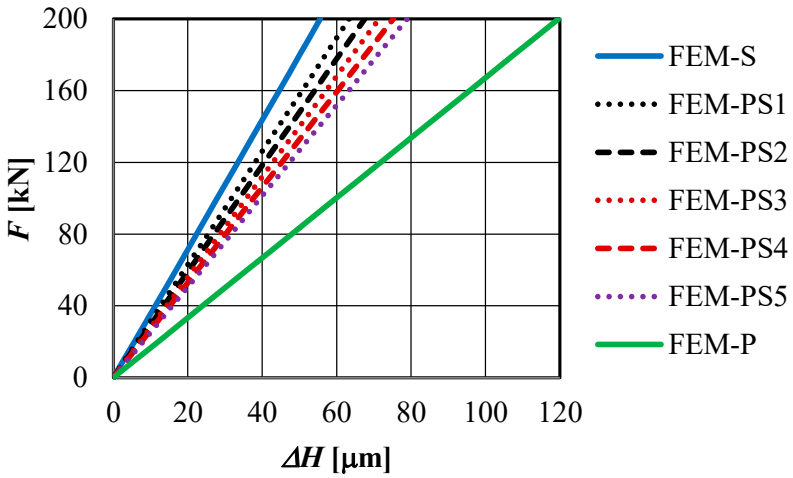

Figure 7. The stiffness characteristics of the components joined in the multi-bolted foundation connection.

In the second step, the total displacements in the Z0X plane of the connected elements in the multi-bolted foundation connection ΔH were determined, corresponding to the maximum load value (F equal to 200 kN). The last parameter adopted for the quantitative comparison of the calculation models is the stiffness of the joined components k, specified as:

$$k = \frac{F}{\Delta H} \quad (1)$$

The stiffness values of the joined components obtained for the adopted multi-bolted foundation connection models are summarised in Table 3.

Table 3. The stiffness values of the components joined in the multi-bolted foundation connection.

Model	FEM-S	FEM-PS1	FEM-PS2	FEM-PS3	FEM-PS4	FEM-PS5	FEM-P
k, kN/μm	3.60	3.15	2.96	2.80	2.66	2.53	1.67

The values of the relative difference ε between the stiffness of the components joined with a steel shim and the stiffness of the components joined with individual polymer–steel shims are shown in Table 4.

Table 4. The relative difference ε values.

Model	FEM-PS1	FEM-PS2	FEM-PS3	FEM-PS4	FEM-PS5
ε, %	12.5	17.8	22.2	26.1	29.7

On the basis of the calculation results for the assumed multi-bolted foundation connection models, it can be stated that the use of polymer–steel shims can result in the following:

1. Significant improvement in the stiffness of the multi-bolted foundation connection in comparison to the connection with a polymer shim;
2. The achievement of a multi-bolted foundation connection with a stiffness close to that of the connection with a steel shim (at a sufficiently low polymer layer thickness).

4. Conclusions

This communication analyses multi-bolted foundation connections made in three ways. The novelty of the communication is the investigation of the effect of the thickness of the polymer layer in the foundation shim on the stiffness of the multi-bolt foundation connection. It is shown that the use of polymer–steel shims can result in a significant

improvement in the stiffness of a multi-bolted foundation connection compared to a connection with a polymer shim (at a sufficiently low polymer layer thickness). It is also shown that a multi-bolted foundation connection with a polymer–steel shim can have stiffness characteristics similar to a multi-bolted foundation connection with a steel shim. Meanwhile, these connections have advantages characteristic of polymer shim connections, the most significant of which is the lack of need for precise machining and close adhesion of the shim to the rough surfaces of the machine and foundation components to be joined over the whole nominal contact area.

Funding: This research received no external funding.

Data Availability Statement: The data presented in this study are available on request from the author.

Conflicts of Interest: The author declares no conflicts of interest.

References

1. Grzejda, R. FE-modelling of a contact layer between elements joined in preloaded bolted connections for the operational condition. *Adv. Sci. Technol. Res. J.* **2014**, *8*, 19–23. [CrossRef]
2. Palenica, P.; Powałka, B.; Grzejda, R. Assessment of modal parameters of a building structure model. *Springer Proc. Math. Stat.* **2016**, *181*, 319–325.
3. Diakun, J. Recycling product model and its application for quantitative assessment of product recycling properties. *Sustainability* **2024**, *16*, 2880. [CrossRef]
4. Krajewski, S.J.; Grochała, D.; Tomków, J.; Grzejda, R. Analysis of the surface stereometry of alloyed austenitic steel after fibre laser cutting using confocal microscopy. *Coatings* **2023**, *13*, 15. [CrossRef]
5. Grochała, D.; Grzejda, R.; Parus, A.; Berczyński, S. The wavelet transform for feature extraction and surface roughness evaluation after micromachining. *Coatings* **2024**, *14*, 210. [CrossRef]
6. Nozdrzykowski, K.; Chybowski, L.; Dorobczyński, L. Model-based estimation of the reaction forces in an elastic system supporting large-size crankshafts during measurements of their geometric quantities. *Measurement* **2020**, *155*, 107543. [CrossRef]
7. Chybowski, L.; Nozdrzykowski, K.; Grządziel, Z.; Dorobczyński, L. Evaluation of model-based control of reaction forces at the supports of large-size crankshafts. *Sensors* **2020**, *20*, 2654. [CrossRef]
8. Nozdrzykowski, K.; Grządziel, Z.; Dunaj, P. Determining geometrical deviations of crankshafts with limited detection possibilities due to support conditions. *Measurement* **2022**, *189*, 110430. [CrossRef]
9. Piaseczny, L. New types of washers and foundation bolts for seating marine diesel engines. *Combust. Engines* **2009**, *48*, 23–27. [CrossRef]
10. Grudziński, P.; Konowalski, K. Experimental investigations of normal deformation characteristics of foundation chocks used in the seating of heavy machines and devices, Part I. Theoretical fundamentals and investigations of a steel chock. *Adv. Manuf. Sci. Technol.* **2014**, *38*, 63–76. [CrossRef]
11. Grudziński, P.; Konowalski, K. Experimental investigations of normal deformation characteristics of foundation chocks used in the seating of heavy machines and devices, Part II. Experimental investigations of a chock cast of EPY resin. *Adv. Manuf. Sci. Technol.* **2014**, *38*, 51–61.
12. Grudziński, K.; Grudziński, P.; Jaroszewicz, W.; Ratajczak, J. Assembling of bearing sleeve on ship propulsion shaft by using EPY resin compound. *Pol. Marit. Res.* **2012**, *19*, 49–55. [CrossRef]
13. Urbaniak, M.; Ratajczak, J. Modernization of foundations for industrial and ship's machines and devices with use of the EPY compound, Part 1. Practical applications of the EPY compound. *Inż. Mater. Mater. Eng.* **2015**, *36*, 532–536. (In Polish)
14. Comer, A.J.; Dhôte, J.X.; Stanley, W.F.; Young, T.M. Thermo-mechanical fatigue analysis of liquid shim in mechanically fastened hybrid joints for aerospace applications. *Compos. Struct.* **2012**, *94*, 2181–2187. [CrossRef]
15. Dhôte, J.X.; Comer, A.J.; Stanley, W.F.; Young, T.M. Study of the effect of liquid shim on single-lap joint using 3D Digital Image Correlation. *Compos. Struct.* **2013**, *96*, 216–225. [CrossRef]
16. Liu, L. The influence of the substrate's stiffness on the liquid shim effect in composite-to-titanium hybrid bolted joints. *Proc. Inst. Mech. Eng. Part G J. Aerosp. Eng.* **2014**, *228*, 470–479. [CrossRef]
17. Dhôte, J.X.; Comer, A.J.; Stanley, W.F.; Young, T.M. Investigation into compressive properties of liquid shim for aerospace bolted joints. *Compos. Struct.* **2014**, *109*, 224–230. [CrossRef]
18. Yue, X.; An, L.; Chen, Z.; Wang, C.; Cai, Y.; Xiao, R. Influence of gap filling on mechanical properties of composite-aluminum single-lap single-bolt hybrid joints. *Adv. Mech. Eng.* **2021**, *13*, 16878132241254181. [CrossRef]
19. Yue, X.; An, L.; Chen, Z.; Cai, Y.; Wang, C. Effect of preload and shim types on the mechanical properties of composite-aluminium bolted joints. *Proc. Inst. Mech. Eng. Part C J. Mech. Eng. Sci.* **2022**, *236*, 1099–1118. [CrossRef]

20. Okorn, I.; Nagode, M.; Klemenc, J.; Oman, S. Influence of geometric imperfections of flange joints on the fatigue load of preloaded bolts. *Int. J. Press. Vessel. Pip.* **2024**, *210*, 105237. [CrossRef]
21. Wysmulski, P. The effect of load eccentricity on the compressed CFRP Z-shaped columns in the weak post-critical state. *Compos. Struct.* **2022**, *301*, 116184. [CrossRef]
22. Wysmulski, P. Numerical and experimental study of crack propagation in the tensile composite plate with the open hole. *Adv. Sci. Technol. Res. J.* **2023**, *17*, 249–261. [CrossRef]
23. Wysmulski, P. Analysis of the effect of an open hole on the buckling of a compressed composite plate. *Materials* **2024**, *17*, 1081. [CrossRef] [PubMed]
24. Wysmulski, P.; Mieczkowski, G. Influence of size of open hole on stability of compressed plate made of carbon fiber reinforced polymer. *Adv. Sci. Technol. Res. J.* **2024**, *18*, 238–247. [CrossRef]
25. Nesbitt, B. How to support your pump and associated equipment. *World Pumps* **2002**, *2002*, 26–29. [CrossRef]
26. Geitner, F.K.; Bloch, H.P. *Machinery Component Maintenance and Repair*, 4th ed.; Gulf Professional Publishing: Houston, TX, USA, 2019.
27. Piaseczny, L. Designing of power plant rechocking using a pourable polymer on example of ship's power plant. *Eksploat. Niezawodn. Maint. Reliab.* **2002**, *4*, 26–38.
28. Żach, P. Composite materials in special machine applications. *Tworz. Sztucz. Chem.* **2005**, *5*, 16–19. (In Polish)
29. Kawiak, M.; Kawiak, R. Material selection for foundation chocks of machines. *Inż. Mater. Mater. Eng.* **2015**, *36*, 528–531. (In Polish)
30. Grudziński, P.; Konowalski, K. Studies of flexibility of a steel adjustable foundation chock. *Adv. Manuf. Sci. Technol.* **2012**, *36*, 79–90.
31. Yongsheng, Z.; Nana, N.; Hongyan, C.; Ying, L.; Kai, J.; Lingjun, M. Calculation method of the contact stiffness of bed-foundation interfaces considering foundation creep. *J. Braz. Soc. Mech. Sci. Eng.* **2021**, *43*, 427. [CrossRef]
32. Piaseczny, L. Marine engine seating on polymer-metal chocking. *Combust. Engines* **2008**, *47*, 3–13. [CrossRef]
33. Wald, F.; Vild, M.; Kuříková, M.; Kabeláč, J.; Sekal, D.; Maier, N.; Da Silva Seco, L.; Couchaux, M. Component based finite element design of steel joints. *Civ. Eng. Des.* **2020**, *2*, 78–89. [CrossRef]
34. Nawar, M.T.; Matar, E.B.; Maaly, H.M.; Alaaser, A.G.; El-Zohairy, A. Assessment of rotational stiffness for metallic hinged base plates under axial loads and moments. *Buildings* **2021**, *11*, 368. [CrossRef]
35. Saleem, S.; Hejazi, F.; Ostovar, N. Health monitoring of ultra high fiber performance reinforced concrete communication tower using machine learning algorithms. *J. Civ. Struct. Health Monit.* **2023**, *13*, 1105–1130. [CrossRef]
36. Tanlak, N.; Sonmez, F.; Talay, E. Detailed and simplified models of bolted joints under impact loading. *J. Strain Anal. Eng. Des.* **2011**, *46*, 213–225. [CrossRef]
37. Díaz, C.; Martí, P.; Victoria, M.; Querin, O.M. Review on the modelling of joint behaviour in steel frames. *J. Constr. Steel Res.* **2011**, *67*, 741–758. [CrossRef]
38. Grzejda, R. New method of modelling nonlinear multi-bolted systems. In *Advances in Mechanics: Theoretical, Computational and Interdisciplinary Issues*, 1st ed.; Kleiber, M., Burczyński, T., Wilde, K., Gorski, J., Winkelmann, K., Smakosz, Ł., Eds.; CRC Press: Leiden, The Netherlands, 2016; pp. 213–216.
39. Kim, J.; Yoon, J.-C.; Kang, B.-S. Finite element analysis and modeling of structure with bolted joints. *Appl. Math. Model.* **2007**, *31*, 895–911. [CrossRef]
40. Shan, M.; Zhao, L.; Huang, W.; Liu, F.; Zhang, J. Effect mechanisms of hygrothermal environments on failure of single-lap and double-lap CFRP-aluminum bolted joints. *Comput. Model. Eng. Sci.* **2020**, *123*, 101–127.
41. Tartaglia, R.; D'Aniello, M.; Zimbru, M. Experimental and numerical study on the T-Stub behaviour with preloaded bolts under large deformations. *Structures* **2020**, *27*, 2137–2155. [CrossRef]
42. Mahaarachchi, D.; Mahendran, M. Finite element analysis and design of crest-fixed trapezoidal steel claddings with wide pans subject to pull-through failures. *Eng. Struct.* **2004**, *26*, 1547–1559. [CrossRef]
43. Oskouei, R.H.; Keikhosravy, M.; Soutis, C. Estimating clamping pressure distribution and stiffness in aircraft bolted joints by finite-element analysis. *Proc. Inst. Mech. Eng. Part G J. Aerosp. Eng.* **2009**, *223*, 863–871. [CrossRef]
44. Razavi, H.; Abolmaali, A.; Ghassemieh, M. Invisible elastic bolt model concept for finite element analysis of bolted connections. *J. Constr. Steel Res.* **2007**, *63*, 647–657. [CrossRef]
45. Schaumann, P.; Kleineidam, P.; Seidel, M. FE-modelling of connections with bolts in tension. *Stahlbau* **2001**, *70*, 73–84. (In German) [CrossRef]
46. Bouzid, A.-H.; Beghoul, H. The Design of Flanges Based on Flexibility and Tightness. In *Analysis of Bolted Joints, Proceedings of the 2003 ASME Pressure Vessels and Piping Conference, Cleveland, OH, USA, 20–24 July 2003*; ASME: New York City, NY, USA, 2003; pp. 31–38.
47. Grudziński, P. Deformation and stress analysis of foundation bolted joints, Part 2: A foundation bolted joint with a chock made of plastic. *Model. Inż.* **2014**, *21*, 72–79. (In Polish)
48. Grudziński, K.; Jaroszewicz, W.; Grudziński, P.; Ratajczak, J. 40 years in application of Polish resins in the seating of machines and devices on foundations. *Prz. Mech.* **2015**, *74*, 26–35. (In Polish)

49. Midas NFX, Analysis Manual. Available online: https://www.dropbox.com/s/10g192o8chk0plq/midas%20NFX%20Analysis%20Manual.pdf?dl=1 (accessed on 29 August 2024).
50. Grzejda, R. Designation of a normal stiffness characteristic for a contact joint between elements fastened in a multi-bolted connection. *Diagnostyka* **2014**, *15*, 61–64.